Dyes and Pigments 93 (2012) 1447–1455

Contents lists available at SciVerse ScienceDirect

Dyes and Pigments

journal homepage: www.elsevier.com/locate/dyepig

A novel fluorescein-based dye containing a catechol chelating unit to sense iron(III)

Carla Queirós [a], Ana M.G. Silva [b,*], Sílvia C. Lopes [b], Galya Ivanova [b], Paula Gameiro [b], Maria Rangel [a,*]

[a] REQUIMTE, Instituto de Ciências Biomédicas de Abel Salazar, 4099-003 Porto, Portugal
[b] REQUIMTE, Departamento de Química, Faculdade de Ciências, Universidade do Porto, Rua do Campo Alegre, 4169-007 Porto, Portugal

ARTICLE INFO

Article history:
Received 27 June 2011
Received in revised form
25 September 2011
Accepted 9 October 2011
Available online 20 October 2011

Keywords:
Catechol
Fluorescein
Chemosensor
Fluorescence spectroscopy
Iron(III)
Microwave irradiation

ABSTRACT

In the present work we report the synthesis and characterization of a novel fluorescein-based dye containing a catechol chelating unit designed to act as a chemosensor for iron(III). The compound was prepared using conventional and microwave-assisted amide coupling of a catechol derivative with a 5(6)-carboxyfluorescein scaffold. One of the most interesting features of this conjugate structure is a high affinity binding site on the catechol ring close to the fluorophore. As a consequence, the behaviour of the new compound in the presence of metal ions of biological importance was monitored by optical spectroscopy (at physiological pH). The results show that the conjugate is particularly sensitive to iron(III), thus suggesting that it may be used as fluorescent chemosensor for the detection of iron(III) in cellular systems.

1. Introduction

There is an increasing interest in the design of fluorescent chemosensors to detect biologically important metal ions, such as zinc(II), iron(III) and copper(II) [1–4]. According to Czarnik, a fluorescent chemosensor is a conjugate incorporating a binding site, a fluorophore (fluorescent dye) and a mechanism that allows communication between the two [5]. Based on this concept, fluorescent chemosensors have been widely used in the construction of fluorescence devices for chemical, biological and medicinal applications [6,7]. These fluorescence devices are an alternative method to laborious analytical techniques, since they allow not only the *in situ* and real time detection but also analyte quantification at lower cost [8].

Xanthenes, for example fluorescein, are one of the most common classes of fluorophores used for iron(III) [9], copper(II) [10] and zinc(II) [11] fluorescent chemosensors. This fact is due to the excellent photophysical properties of fluorescein namely, high molar absorptivity, intense fluorescent spectrum in the visible region, high quantum yield and photostability [12]. In addition, different functionalities can be introduced on the fluorescein scaffold in order to supply a selective and sensitive receptor site for each metal ion [13]. Specifically, we are focusing our attention on catechol derivatives as receptors mainly because of their intrinsic acid–base properties ($pK_a = 9.2$ and 13.0 for catechol in water) [14]. Catechol-containing molecules are of widespread biological occurrence and importance [15]. It is worth to mention that catechol groups are the chelating moieties of various siderophores and make up the main structure of catecholamines. The latter compounds are of pharmacological use in fields such as: Parkinson's disease treatment [16] and hypertension [17] in addition to their physiological action as neurotransmitters. Catecholate compounds can also be used in breast cancer therapies [18].

Iron represents an essential trace element holding a central position in virtually all organisms as the physiologically most abundant and versatile transition metal [19]. Taking into account the biological relevance of iron and the need to access the element within the cell a series of fluorescent iron(III) chelators bearing a fluorescein function covalently bound to a 3-hydroxy-4-pyridinone unit have been synthesised [20,21]. Some of these fluorescent iron chelators were used to determine labile iron in primary hepatocytes [22,23].

Here, we describe the synthesis and photophysical properties of a fluorescein-based dye containing a catechol chelating unit (**Cat1**, Scheme 1) close to the fluorophore. The catechol unit exhibits a very high affinity for iron(III) and consequently this newly prepared conjugate can be used as a highly efficient chemosensor for iron(III).

* Corresponding authors.
E-mail addresses: ana.silva@fc.up.pt (A.M.G. Silva), mcrangel@fc.up.pt (M. Rangel).

0143-7208/$ – see front matter © 2011 Elsevier Ltd. All rights reserved.
doi:10.1016/j.dyepig.2011.10.010

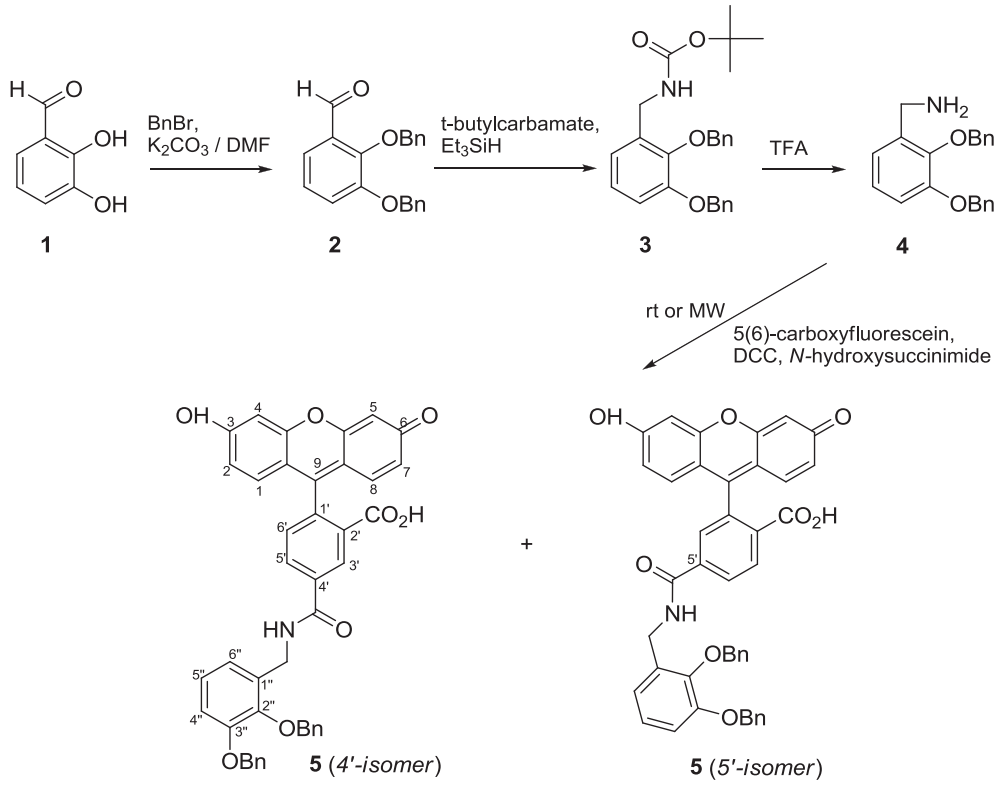

Scheme 1. Synthetic approach to synthesise conjugate **5**.

2. Experimental

2.1. Materials and instruments

Reagents and solvents were purchased as reagent-grade and used without further purification unless otherwise stated.

NMR spectra were recorded on a Bruker Avance III 400, operating at 400.15 MHz for protons and 100.62 MHz for carbons, equipped with pulse gradient units, capable of producing magnetic field pulsed gradients in the *z*-direction of 50.0 G/cm. NMR spectra were acquired in deuterated methanol or deuterated chloroform at 300 K. Two-dimensional $^{1}H/^{1}H$ correlation spectra (COSY), gradient selected $^{1}H/^{13}C$ heteronuclear single quantum coherence (HSQC) and $^{1}H/^{13}C$ heteronuclear multiple bond coherence (HMBC) spectra were acquired using the standard Bruker software. Mass spectra were acquired by Unidade De Espectrometria De Masas of Santiago de Compostela and microanalyses were acquired by Unidad De Análisis Elemental of Santiago de Compostela. Flash chromatography was carried out using silica gel Merck (230–400 mesh).

Electronic absorption spectra were recorded on a Shimadzu–UV 3600 UV–Vis–NIR Spectrophotometer, equipped with a Varian Cary single cell Peltier accessory and fluorescence measurements were performed with a Varian Cary Elipse Spectrofluorometer equipped with a multicell cell holder. For the spectrophotometric titrations we used a Crison pH meter Basic 20^{+} equipped with a combined glass electrode, (cod. 50 29), and standardized at 25 °C using standard buffers of pH 4, 7 and 9.

2.2. Synthesis

2.2.1. Synthesis of 2,3-dibenzyloxybenzaldehyde (2)

To a solution of 2,3-dihydroxybenzaldehyde **1** (1.00 g, 7.24 mmol) and K_2CO_3 (2.20 g, 15.9 mmol) in DMF (20 mL) at 0 °C, benzyl bromide (1.89 mL, 15.9 mmol) was added drop-by-drop, under argon atmosphere. After stirring at 0 °C for 15 min, the reaction mixture was allowed to warm up to room temperature and the stirring was maintained for 4 h. After that time, the reaction mixture was precipitated into an ice–water mixture and neutralized using citric acid. The white solid obtained was filtered, washed with water, dissolved in chloroform and crystallized in *n*-hexane to afford **2** (1.72 g, 75% yield). ^{1}H NMR ($CDCl_3$, 400.15 MHz) δ: 5.19 and 5.20 (2s, 4H, 2xCH_2), 7.12 (dt, 1H, $J = 8.0$ Hz and $J = 0.6$ Hz, H–Ar), 7.23–7.26, 7.32–7.43 and 7.47–7.49 (3*m*, 12H, H–Ar), 10.26 (*s*, 1H, CHO). ^{13}C NMR ($CDCl_3$, 100.62 MHz) δ: 71.3 (CH_2), 76.5 (CH_2), 119.6, 119.9, 124.2, 127.6, 128.3, 128.5, 128.6, 128.7, 128.8, 130.5, 136.3, 151.5, 152.1, 190.2 (CHO); MS (EI) *m*/*z*: 318 $(M)^{+}$. Anal. Calcd for $C_{21}H_{18}O_3$ 1/4H_2O: C, 78.12; H, 5.78; Found: C, 78.46; H, 5.34.

2.2.2. Synthesis of tert-butyl-2,3-dibenzyloxybenzylcarbamate (3)

A solution of 2,3-dibenzyloxybenzaldehyde **2** (1.00 g, 3.14 mmol), *t*-butylcarbamate (1.11 g, 9.43 mmol), triethylsilane, Et_3SiH, (1.50 mL, 9.43 mmol), trifluoroacetic acid (0.47 mL, 6.30 mmol) in acetonitrile (40 mL) was stirred at 22 °C for 5 h. The reaction mixture was precipitated into an aqueous saturated solution of $NaHCO_3$. The resulting white solid was filtered, washed with water and dried in vacuum. Compound **3** was obtained as a white solid (1.26 g) in 93% yield. ^{1}H NMR ($CDCl_3$, 400.15 MHz) δ: 1.42 (*s*, 9H, CH_3), 4.23 (*d*, 2H, $J = 5.9$ Hz, $C\underline{H}_2NH$), 4.75–4.80 (*m*, 1H, NH_2), 5.07 and 5.14 (2*s*, 4H, 2x$C\underline{H}_2C_6H_5$), 6.90–7.03 (*m*, 3H, H–Ar), 7.31–7.37 (*m*, 10H, 2x$CH_2C_6\underline{H}_5$). ^{13}C NMR ($CDCl_3$, 100.62 MHz) δ: 28.4 (CH_3), 40.1 ($\underline{C}H_2NH$), 70.9 (CH_2), 74.9 (CH_2), 113.6, 121.7, 124.2, 127.5, 128.0, 128.2, 128.3, 128.5, 128.59, 128.63, 133.3, 136.9, 137.4, 146.2, 151.7, 155.8 (C=O). Anal. Calcd for $C_{26}H_{29}NO_4$ ½CH_2Cl_2: C, 68.90; N, 3.03; H, 6.55; Found: C, 68.98; N, 2.67; H, 6.04.

2.2.3. Synthesis of 2,3-dibenzyloxybenzylamine (4)

A solution of **3** (1.26 g, 3.01 mmol) in trifluoroacetic acid (1.5 mL) was stirred at 22 °C for 15 min. After that time, the reaction mixture

was neutralized using an aqueous saturated solution of $NaHCO_3$. The resulting solid was filtered, washed with water, dried and purified by flash chromatography using chloroform as eluent to remove a small amount of unchanged starting material and a mixture of chloroform/methanol (9:1) to obtain compound **4** (0.73 mg, 78%). ^{1}H NMR ($CDCl_3$, 400.15 MHz) δ: 3.74 (*s*, 2H, $C\underline{H}_2NH_2$), 5.08 and 5.12 (2*s*, 2H, 2x$C\underline{H}_2C_6H_5$), 6.85 (dd, 1H, J = 7.3 and J = 1.8 Hz, Ar–H), 6.95 (dd, 1H, J = 8.2 and J = 1.8 Hz, Ar–H), 6.99 (dd, 1H, J = 8.2 and J = 7.3 Hz, Ar–H), 7.28–7.46 (*m*, 10H, 2x$CH_2C_6\underline{H}_5$). ^{13}C NMR ($CDCl_3$, 100.62 MHz) δ: 40.3 ($\underline{C}H_2NH_2$), 70.9 (CH_2), 75.0 (CH_2), 113.9, 121.5, 124.4, 127.5, 128.1, 128.3, 128.4, 128.5, 128.60, 128.63, 134.0, 136.7, 137.2, 145.9, 151.7. HRMS-EI: calcd. for $C_{21}H_{21}NO_2$ $(M)^{+\cdot}$ 319.1572; Found 319.1564.

2.2.4. Synthesis of conjugate (5)

a) using standard conditions: *N,N′*-dicyclohexylcarbodiimide (DCC) (1.081 g, 5.24 mmol) and *N*-hydroxysuccinimide (0.603 g, 5.24 mmol) were added to a solution of 5(6)-carboxyfluorescein (1.517 g, 4.03 mmol) in dried DMF (4 mL) were added. The reaction solution was stirred at room temperature overnight (16 h), under argon atmosphere, to complete the intermediate formation of the activated ester. Subsequently, the resulting white precipitate was filtered off and an amount of **4** (1.545 g, 4.84 mmol) was added to the filtrate. The mixture was stirred at room temperature for 24 h, followed by solvent removal under reduced pressure. The resulting residue was taken up in chloroform and the pH was adjusted with a solution of hydrochloric acid (10%) to pH 3 and extracted with a mixture of chloroform/methanol (8:2). After dried under high vacuum, the crude product was purified by chromatography column using a mixture of chloroform/methanol (8.5:1.5) as eluent. Conjugate **5** (0.180 g) was obtained in 27% yield.

b) using microwave irradiation: A mixture of 5(6)-carboxyfluorescein (97.1 mg, 0.258 mmol), DCC (58.1 mg, 0.282 mmol), *N*-hydroxysuccinimide (32.4 mg, 0.282 mmol), **4** (75.0 mg, 0.235 mmol) and dried DMF (2 mL) was placed in a 10 mL reaction vial, which was then closed under argon atmosphere and placed in the cavity of a CEM microwave reactor. The reaction vial was irradiated (1 min ramp to 55 °C and 60 min hold at 55 °C, using 100 W maximum power). The reaction work-up was similar to the described before affording 14.5 mg of conjugate **5** (26% yield). ^{1}H NMR (4′- and 5′-isomers, MeOD, 400.15 MHz) δ: 4.49 and 4.62 (2s, CH_2NH), 5.00, 5.11, 5.13 and 5.18 (4*s*, $CH_2C_6H_5$), 6.53 (dd, *J* 8.8 and *J* 2.3 Hz, H–Ar), 6.60 (*d*, *J* 8.8 Hz, H–Ar), 6.68 (*d*, *J* 2.3 Hz, H–Ar), 6.85 (dd, *J* 8.0 and *J* 1.6 Hz, H–Ar), 6.95–7.57 (*m*, H–Ar), 8.04 (*d*, *J* 8.1 Hz, H–Ar), 8.08 (dd, *J* 8.1 and *J* 1.2 Hz, H–Ar), 8.15 (dd, *J* 8.1 and *J* 1.2 Hz, H–Ar), 8.40 (*s*, H–Ar). ^{13}C NMR (MeOD, 100.62 MHz) δ: 40.1 (CH_2NH), 72.0, 75.8 and 75.9 ($CH_2C_6H_5$), 103.6, 114.8, 122.0, 122.2, 125.37, 125.42, 128.9, 129.0, 129.1, 129.3, 129.4, 129.6, 129.7, 130.3, 130.4, 133.3, 133.5, 137.8, 138.50, 138.54, 138.9, 139.0, 147.27, 147.3, 153.2, 153.3, 168.4 (CONH), 170.6 (COOH). MS (ESI) *m/z*: 678 $(M + H)^+$.

2.2.5. Synthesis of ***Cat1***

A solution of conjugate **5** (228 mg, 0.337 mmol) in methanol (5 mL) and HCl (0.01 mL) was placed into a hydrogenation vessel. The air was displaced with N_2, a catalytic amount of 10% Pd/C (w/w) was added and the mixture was stirred at room temperature, with H_2 at 5 bar for 7 h. The reaction mixture was filtered and the solvent evaporated in vacuum to give the crude product. The resulting residue was crystallized in methanol/chloroform to give 93.8 mg (56% yield). ^{1}H NMR see Table 1 in Supporting Information. HRMS (ESI–TOF): calcd. for $C_{28}H_{22}NO_8$ $(M + H)^+$ 500.1345; Found 500.1340.

2.3. Spectrophotometric measurements

Electronic absorption spectra were recorded using quartz cells with 1 cm path length.

Acidity constants of 2,3-dihydroxybenzaldehyde(**1**) and **Cat1** – 50 μM each – were obtained in aqueous solution prepared in double de-ionized water (conductivity less than 0.1 μS cm^{-1}), by dilution of the DMSO stock solution of **Cat1** (DMSO percentage in the final aqueous solution was always kept less than 1% of the total volume), and with final ionic strength 0.1 M NaCl. After each pH adjustment, with strong acid or base, the solution was transferred into the cuvette, and the absorption spectra were recorded. Spectra were acquired between 225 and 650 nm (1 nm resolution), at 25 °C. A typical experiment included more than 10 solutions in which, at least, 10 different pH values were fixed, in a range between 3 and 12 for **1** and 2–13 for **Cat1**. The pK_a values were determined by using the program pHab 2006 [24] and the associated errors were determined using the Albert and Sergeant theory [25]. The species distribution curves were plotted with the HySS 2009 program [26].

2.4. Fluorescence measurements

Cat1 fluorescence emission measurements were performed in 1 cm cuvettes and all the spectra were recorded at 25.0 ± 0.1 °C, with excitation and emission slit widths of 5 nm, with λ_{exc} = 493 nm and in the range 495–750 nm.

Stock solutions of **Cat1** were obtained by preparing a concentrated solution in DMSO. Samples for the pH dependence of the emission fluorescence intensity study, in a pH range of 2–13, were prepared by dilution of a known volume of the DMSO stock solution in water, to a final concentration of 5 μM and final ionic strength 0.1 M NaCl. Solution's pH was adjusted by adding small aliquots of strong acid or base and DMSO percentage in the final aqueous solution was always kept less than 1% of the total volume.

2.5. Fluorescence quenching

Fluorescence quenching measurements were performed in MOPS buffer (pH 7.4) at 25 °C. Stock solutions of the different metal ions were acquired [$Fe(NO_3)_3$, $Al(NO_3)_3$, $Cu(NO_3)_2$ and $Zn(NO_3)_2$] from Sigma–Aldrich and stabilized with nitrilotriacetic acid trisodium salt (NTA) at a 1:5 proportion. Once again **Cat1** solution was prepared by dilution, of a known volume of the DMSO stock solution, in MOPS buffer to achieve a final 3 μM concentration of **Cat1**. DMSO's percentage in the final aqueous solution was always kept less than 1% of the total volume. The ligand solution was then mixed with increasing amounts of the metal stock solution, in a range of molar ratios from 10:1 to 1:2 of **Cat1** to metal ion. Fluorescence intensities were always corrected for dilution.

The fluorescence quantum yield values for **Cat1** and 5(6)-carboxyfluorescein were determined, at 25 °C, according to the method of Williams et al. [27] and what is described by Fery-Forgues and Lavabre [28], using fluorescein as standard [29]. To minimize reabsorption effects, the absorbance's sample values were kept below 0.1 [30].

3. Results and discussion

3.1. Synthesis

To synthesise the target fluorescein-based dye functionalized with a catechol unit (**Cat1**) we firstly prepared an *ortho* substituted

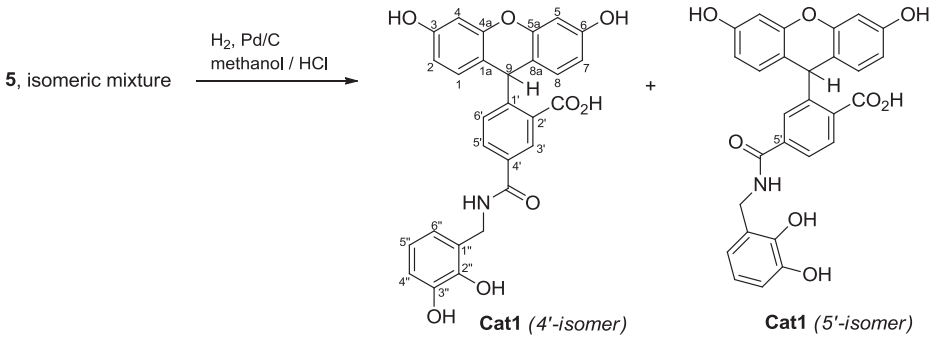

Scheme 2. Synthetic approach to synthesise **Cat1**.

catechol (1,2-dihydroxybenzene) bearing a methylamine group. The synthesis is outlined in Scheme 1 and involves (i) benzylation of the hydroxyl groups of the 2,3-dihydroxybenzaldehyde with benzyl bromide followed by (ii) condensation with *tert*-butylcarbamate, in the presence of triethylsilane and subsequent (iii) hydrolysis in TFA, using a reductive amination protocol [31]. Using this step's sequence, catechol derivative **4** was synthesised in a good yield (82%).

In order to optimize the conditions to perform the coupling reaction of **4** with 5(6)-carboxyfluorescein several procedures have been attempted. Firstly, this reaction was carried out through *in situ* generation of the corresponding activated ester using DCC and *N*-hydroxysuccinimide as coupling reagents and dried DMF as solvent. After stirring at room temperature for 40 h, in argon atmosphere, the reaction provided the desired fluorescein-catechol conjugate **5** in 27% yield. Taking into account the dielectric properties of the reaction solvent (DMF), we anticipated that microwave irradiation could be a good alternative process to improve the reaction performance. In fact, when the same reaction was performed in only 60 min at 55 °C using a microwave monomode apparatus as heating source, the expected conjugate **5** was obtained in 26% yield. This represents a significant reducing of reaction time, from 40 h to 60 min, keeping a similar reaction yield.

In order to obtain the final compound **Cat1**, conjugate **5** was dissolved in a mixture of methanol/HCl and placed under a hydrogen atmosphere over 10% Pd/C. Under these conditions, a yellow powder was isolated which was very soluble in alcoholic solvents, such as methanol and ethanol, but insoluble in water. Its NMR spectra, obtained in methanol-d_4, are consistent with the **Cat1** conjugate (Scheme 2), which results both on the benzyl protecting groups removal and simultaneous reduction of the double bond at position 9 of the xanthene ring.

Taking into account previous work with 3,4-HPOs/naphthalene conjugates [32] this result wasn't expected under these reaction conditions. However, a similar result was described in the literature for a nitro fluorescein derivative using the Raney-Ni reagent as reduction agent [33]. In order to validate our result, we performed the same reaction using the starting material 5(6)-carboxyfluorescein. A reduction on the double bond in position 9 of fluorescein was achieving, as it was confirmed by the presence of the 9-H proton at *ca.* 6.20 ppm correlated with 9-C carbon at *ca.* 40 ppm, in NMR spectra. These chemical shift values were in agreement with the chemical shifts observed for the parent nitro fluorescein derivative, where proton H-9 appears at 6.15 ppm [33].

3.2. NMR spectroscopy

NMR spectroscopy was of particular importance for the structural elucidation of the synthesised compounds (see Fig. 1). The ^{1}H NMR spectrum of the catechol derivative **4** in chloroform-d (A, Fig. 1) shows (i) one singlet at δ 3.74 ppm from $C\underline{H}_2NH_2$ (ii) two singlets at δ 5.08 and 5.12 ppm from CH_2 of the benzyl groups (iii) three double doublets at δ 6.85, 6.95 and 6.99 ppm corresponding to the catechol scaffold protons and (iv) one multiplet at δ 7.28–7.46 ppm corresponding to the aromatic benzyl group protons. Once performed the coupling reaction of **4** with the commercial available 5(6)-carboxyfluorescein, the resulting conjugate **5** was isolated as a 4′- and 5′-isomeric mixture. Thus, for these isomers, the ^{1}H NMR spectrum in methanol-d_4 (B, Fig. 1) revealed to be more complex and the most characteristic signals are (i) a set of two singlets at δ 4.49 and 4.62 ppm attributed to the $C\underline{H}_2NH$ protons, (ii) a set of four singlets at δ 5.00, 5.11, 5.13 and 5.18 ppm from CH_2 of the benzyl groups and (iii) three set of aromatic signals at δ 6.52–6.68, 6.84–7.56 and 8.03–8.40 ppm corresponding to fluorescein and catechol scaffolds. Comparing with the ^{1}H NMR spectra of 4′- and 5′- isomeric mixture of **Cat1,** also in methanol-d_4 (C, Fig. 1), the most interesting differences observed are (i) the absence of the resonance of the benzyl groups and (ii) the appearing of a group of two singlets at δ 6.19 and 6.30 ppm attributed to the resonance of H-9 protons.

The ^{1}H and ^{13}C NMR signal assignment of **Cat1** (available in the Supporting Information) was achieved by analysis of ^{1}H/^{1}H COSY,

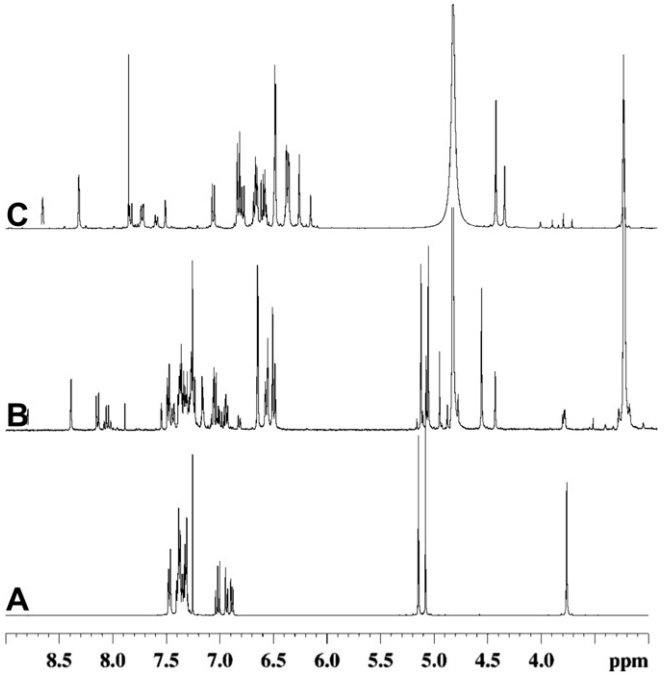

Fig. 1. ^{1}H NMR spectra (A) **4**, (B) 4′- and 5′- isomeric mixture of conjugate **5**, (C) 4′- and 5′- isomeric mixture of **Cat1**.

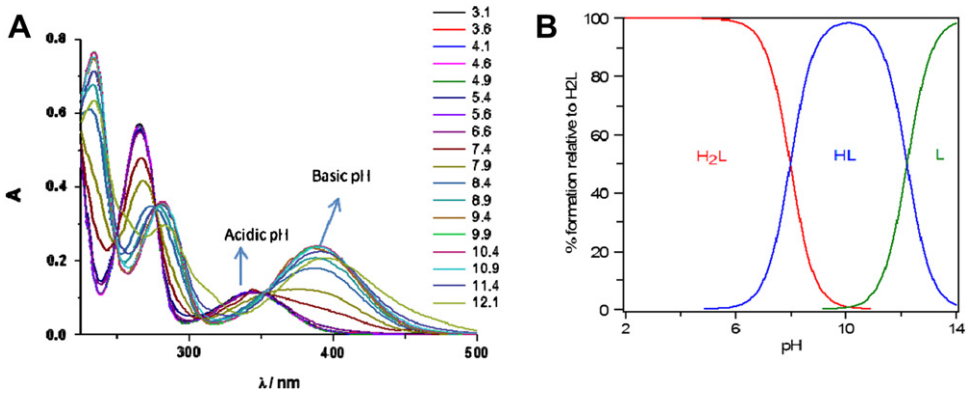

Fig. 2. (A) UV–Vis spectra of 2,3-dihydroxybenzaldehyde in the pH range 2–12. [2,3-dihydroxybenzaldehyde] = 50 μM, 0.1 M NaCl, 25 °C. (B) Speciation diagram of 2,3-dihydroxybenzaldehyde as a function of pH.

$^1H/^{13}C$ HSQC and $^1H/^{13}C$ HMBC spectra and the determined structures are presented in Scheme 2. Well separated resonance signals were observed in all spectra for both isomeric forms (4′- isomer and 5′ -isomer) and their structures were defined by analysis of the ^1H NMR spectrum and the results verified by $^1H/^1H$ COSY and $^1H/^{13}C$ HMBC spectra. The mole ratio of 4′- and 5′ -isomers was found to be 1:0.5 as it was determined from the integral intensity of their characteristic resonance signals in ^1H NMR spectrum. The tentative assignment of the proton and carbon chemical shifts at position 9 in the molecules was proved on the basis of the multiple bonds $^1H–^{13}C$ connectivity's observed in $^1H/^{13}C$ HMBC spectrum (See Supporting Information). Well resolved cross peaks due to long range CH couplings (^3JCH) were observed between the proton at 6.30 ppm (H-9) and carbons C-1/8, C-4a/5a, C-1a/8a, C-1′, C-6′ (in both forms). Additionally, long range CH couplings (^3JCH) were registered between C-9 (38.7 ppm) and the aromatic protons H-1/8 and H-6′ in both isomer forms. The ^1H and ^{13}C NMR spectral data confirm the structure of the two isomeric forms, presented in Scheme 2.

3.3. *Characterization in aqueous solution of 2,3-dihydroxybenzaldehyde and **Cat1***

The dissociation constants of catechol, 2,3-dihydroxybenzaldehyde, were determined by spectrophotometric titration and used as comparative term for ligand **Cat1**. 2,3-Dihydroxybenzaldehyde possesses two dissociable protons, corresponding to the two hydroxyl groups and the values obtained for these two acidity constants – pK_as (see Table 2) are within the usual ranges observed for catechols [14].

The UV–Vis spectra obtained for 2,3-dihydroxybenzaldehyde in aqueous solution in the pH range 2–12 are depicted in Fig. 2 together with the corresponding speciation diagram.

The spectra depicted in Fig. 2 show a batochromic displacement of the 2,3-dihydroxybenzaldehyde bands with increasing pH. The distribution diagram shows that at physiological pH the species H_2L and (HL^-) are present in approximately identical percentage.

According to the NMR characterization, **Cat1** possesses 5 protonation sites (H_5L, Scheme 3) and the determination of its pK_a values was performed by spectrophotometric titration (the UV–Vis spectra of the pH titration are depicted in Fig. 3).

The spectra shown in Fig. 3 are quite different from those of Fig. 2 showing a strong band at *ca.* 500 nm characteristic of the fluorophore. As pH increases a batochromic displacement of the band is observed.

The acidity constants values determined for **Cat1** (represented as H_5L) are valid under the experimental conditions of this work and the data refinement was performed assuming the proposed model Equations (1)–(5).

$$H_5L(aq) \Leftrightarrow H_4L^-(aq) + H^+(aq) \quad \beta_{0,1,-1,0} \tag{1}$$

$$H_5L(aq) \Leftrightarrow H_3L^{2-}(aq) + 2H^+(aq) \quad \beta_{0,1,-2,0} \tag{2}$$

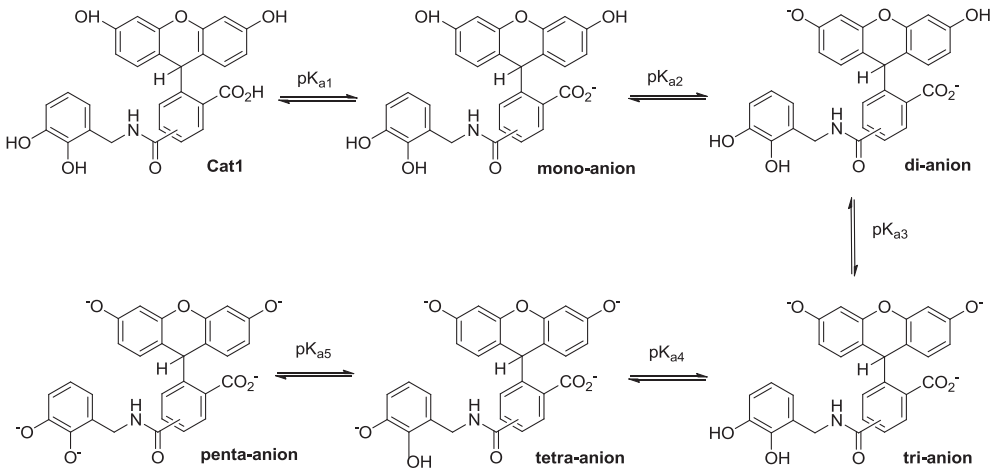

Scheme 3. Proposed protonation sequence of **Cat1**.

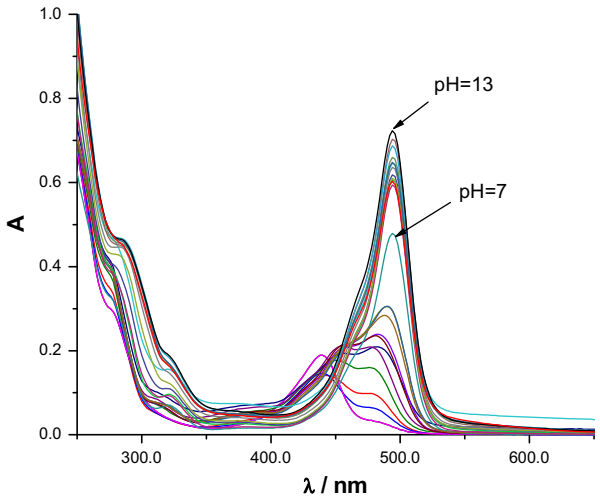

Fig. 3. UV–Vis spectra of **Cat1** in a pH range from 2 to 13 ([**Cat1**] = 50 μM, 0.1 M NaCl, 25 °C).

$$H_5L(aq) \Leftrightarrow H_2L^{3-}(aq) + 3H^+(aq) \quad \beta_{0,1,-3,0} \tag{3}$$

$$H_5L(aq) \Leftrightarrow HL^{4-}(aq) + 4H^+(aq) \quad \beta_{0,1,-4,0} \tag{4}$$

$$H_5L(aq) \Leftrightarrow L^{5-}(aq) + 5H^+(aq) \quad \beta_{0,1,-5,0} \tag{5}$$

The log $\beta_{0,1,-n,0}$ determined are presented in Table 1.

According to the proposed model refinement of data allowed the determination of only four log β values. Therefore we tested new set model equations – Eqs. (6)–(9) -, and from their data refinement we determined the pK_a values of **Cat1**.

$$H_5L(aq) \Leftrightarrow H_4L^{-}(aq) + H^+(aq) \quad \beta_{0,1,-1,0} \tag{6}$$

$$H_5L(aq) \Leftrightarrow H_2L^{3-}(aq) + 3H^+(aq) \quad \beta_{0,1,-3,0} \tag{7}$$

$$H_5L(aq) \Leftrightarrow HL^{4-}(aq) + 4H^+(aq) \quad \beta_{0,1,-4,0} \tag{8}$$

$$H_5L(aq) \Leftrightarrow L^{5-}(aq) + 5H^+(aq) \quad \beta_{0,1,-5,0} \tag{9}$$

The pK_a values of catechol units and the fluorescein scaffold [34] are well documented in literature and are registered in Table 2 together with those determined in this work for 2,3-dihydroxybenzaldehyde and **Cat1**.

In fluorescein derivatives the equilibrium between enol and lactone forms is generally observed [23,34]. However in our case this equilibrium is prevented by the presence of the hydrogen atom at C-9. Taking into account the pK_as obtained it is possible to conclude that: the first pK_{a1} registered in Table 2 for 5(6)-carboxyfluorescein does not exist for **Cat1.** The deprotonation of **Cat1** is related to the hydroxyl groups present in: (i) fluorescein scaffold at carbon atoms C-3, C-6 and C-2′ and (ii) catechol unit at C-2″ and C-3″.

Table 1
Log $\beta_{0,1,-n,0}$ values determined for **Cat1** considering the proposed model equations.

	log $\beta_{0,1,-n,0}$
$\beta_{0,1,-1,0}$	−4.05 ± 0.03
$\beta_{0,1,-2,0}$	−10.18 ± 0.06
$\beta_{0,1,-3,0}$	–
$\beta_{0,1,-4,0}$	−25.76 ± 0.07
$\beta_{0,1,-5,0}$	−35.76 ± 0.08

Table 2
Acidity constants of 5(6)-carboxyfluorescein, 2,3-dihydroxybenzaldehyde and **Cat1**.

pK_{ai}	5(6)-carboxyfluorescein [34]	2,3-dihydroxybenzaldehyde	**Cat1** (H_5L)
pK_{a1}	2.08	7.97 ± 0.01	4.08 ± 0.06
pK_{a2}	4.31	12.22 ± 0.03	12.5 ± 0.1
pK_{a3}	6.43		8.2 ± 0.1
pK_{a4}			10.4 ± 0.1

The pK_a values obtained by UV–Vis spectroscopy show that the pK_a values of the hydroxyl groups of C-3 and C-6 are only observed together, and as a model in the pHab2006 program we had to assume their simultaneous deprotonation thus meaning that the value calculated for pK_{a2} accounts for the "sum" of the two pK_a values. Therefore our results allowed the determination of "four" acidity constants for **Cat1**, which are in agreement with values determined for 5(6)-carboxyfluorescein and 2,3-dihydroxybenzaldehyde. Considering the pK_a values determined for **Cat1** we plotted the correspondent species distribution diagram as a function of pH (Fig. 4). At physiological pH one predominant specie is present, $[H_2L]^{3-}$.

Considering the data obtained (see Table 2) and considering that at pH above 6.43, fluorescein scaffold should be a dianionic species [34], and consequently more soluble in water, it can be expected that be most adequate pH value to study **Cat1** in aqueous media is the physiological one. Considering the protonation scheme proposed, previous published studies [34] and the results obtained for **Cat1** pK_as it should be expected that, at physiological pH, **Cat1** is fully deprotonated in the fluorescein scaffold and protonated at the catechol unit.

In order to study the behaviour of **Cat1** in the presence of metal ions a profile of the variation of fluorescence intensity with pH was obtained (Fig. 5). The results show that the fluorescence intensity increases with the pH reaching a maximum at 7.4.

Considering the results, the potential biological application of **Cat1** and the fluorescent data presented (Fig. 5) which shows that maximum fluorescence intensity is obtained at pH 7.4 we considered **Cat1** as a good candidate to pursue studies of metal ion interaction at physiological pH. Before the latter studies the photophysical characterization of **Cat1** and the fluorophores – fluorescein and 5(6)-carboxyfluorescein – was performed at pH 7.4 and the results namely the λ_{max} for absorption and fluorescence emission, the molar absorption coefficient (ε) and the fluorescence quantum yield (Φ_F) are shown in Table 3.

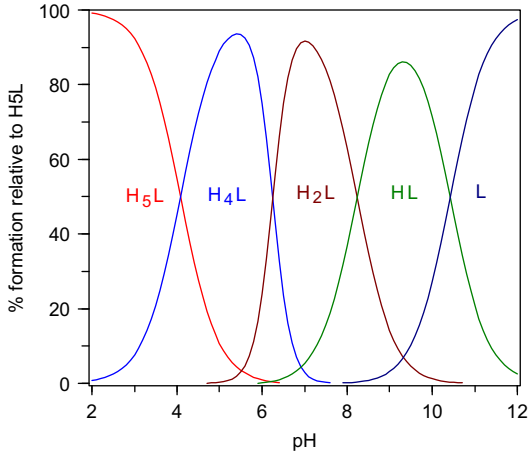

Fig. 4. Distribution diagram of **Cat1** (50 μM, 25 °C) as a function of pH

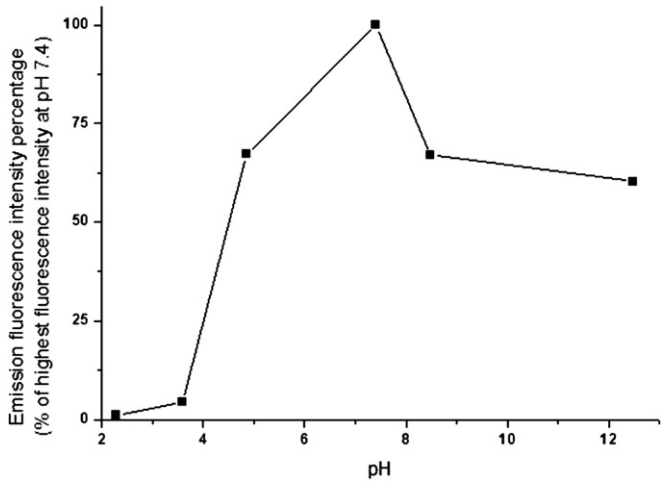

Fig. 5. Graphical representation of emission fluorescence intensity percentage of **Cat1** in a pH range from 2 to 12 (considering 100% of emission fluorescence intensity for pH 7.4).

The Φ_F values determined for **Cat1** and 5(6)-carboxyfluorescein are lower than the standard fluorophore (fluorescein) as expected according to their structures.

3.4. Behaviour of *Cat1* in the presence of metal ions

The interaction of **Cat1** with different metal ions (Fe^{3+}, Al^{3+}, Zn^{2+} and Cu^{2+}) was investigated by examining the variations observed in the fluorescence intensity of the fluorophore. Evidence of the corresponding metal complexes formation in solution can be provided by observation of a significant quenching of fluorescence intensity. Quenching experiments were therefore performed using increasing concentrations of the metal ions and a fixed concentration of **Cat1**. As an example we present in Fig. 6 the emission fluorescence intensity change of **Cat1** with increasing concentrations of Fe(III). The results obtained for the other metal ions tested are similar to this one but less expressive in terms of the emission fluorescence intensity decrease.

From analysis of Fig. 6 we can conclude that the quenching effect of Fe(III) on **Cat1** is almost complete at a ratio 1:3 (metal/ligand) as expected, considering similar studies with 3,4-HPOs [23] and the percentage of fluorescence quenching is *ca.* 70%. For the other metal ions the decrease in the emission fluorescence intensity is: 19% for Al^{3+}, 32% for Cu^{2+} and 4% for Zn^{2+}. A comparison of results obtained for 3 μM solutions of **Cat1** together with a 1:1 M ratio of metal ion is shown in Fig. 7.

Comparing the obtained data with previous results of an equivalent 3,4-HPO ligand [23], we conclude that the percentage of fluorescence quenching of **Cat1** in the presence of Fe(III) is very similar.

Emission fluorescence intensity quenching of **Cat1** in the presence of increasing concentrations of the biologically relevant metal ions Fe^{3+}, Al^{3+}, Zn^{2+} and Cu^{2+} is depicted in Fig. 8. The results show

Table 3
Photophysical parameters (λ_{max} for absorption and fluorescence emission, ε and Φ_F) for **Cat1**, 5(6)-carboxyfluorescein and fluorescein in MOPS, pH 7.4, at 25 °C.

	UV–Vis		Fluorescence	
	λ_{max} (nm)	ε ($\times 10^5$ M^{-1} cm^{-1})	λ_{max} (nm)	Φ_F
Cat1	493	1.45	518	0.55
5(6)-carboxyfluorescein	492	5.78	516	0.70
fluorescein	490	3.10	510	0.78

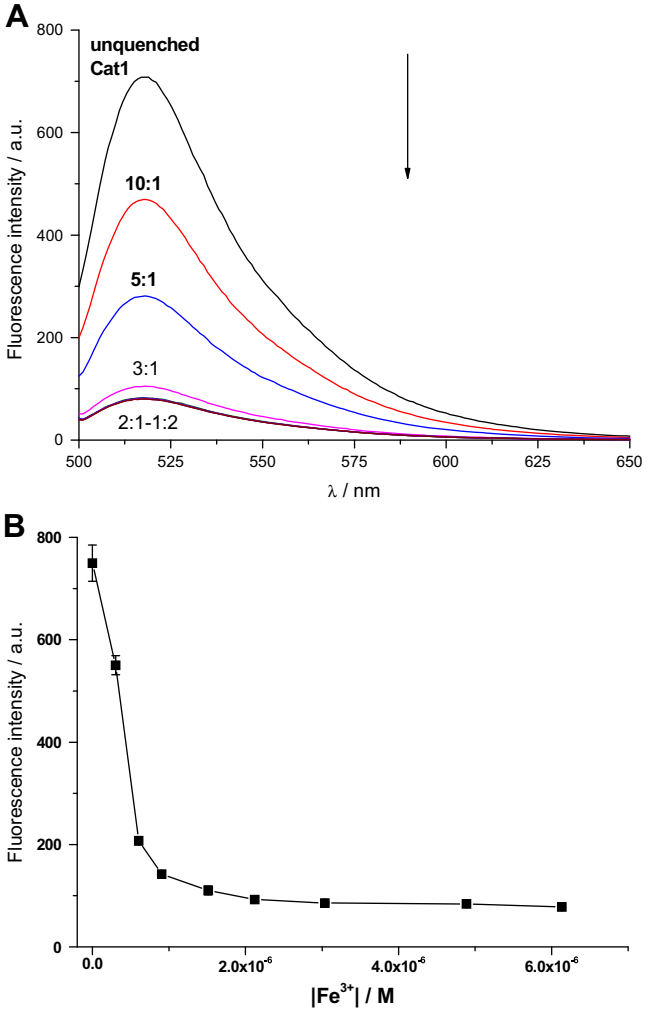

Fig. 6. (A) Graphical representation of **Cat1** (MOPS, pH 7.4, at 25 °C, λ_{exc} = 493 nm) emission fluorescence intensities with increasing Fe(III) concentrations (arrow). **Cat1**/metal ratios of 10:1, 5:1, 3:1, 2:1, 1:1, 1:1.6 and 1:2 were tested. (B) Maximum emission fluorescence intensity (measured at λ_{em} = 518 nm) plotted against corresponding Fe(III) concentrations. Measurements were carried out in triplicate.

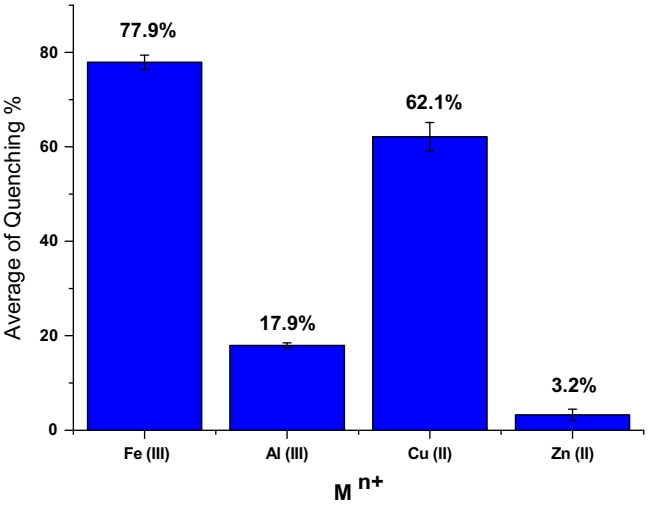

Fig. 7. Influence of Fe^{3+}, Al^{3+}, Cu^{2+} and Zn^{2+} on the emission fluorescence intensity of **Cat1**. The results were obtained in a 3 μM **Cat1** solution (10 mM MOPS, pH 7.4, 25 °C) with a fixed 1:1 M ratio for all the different metal ions understudy.

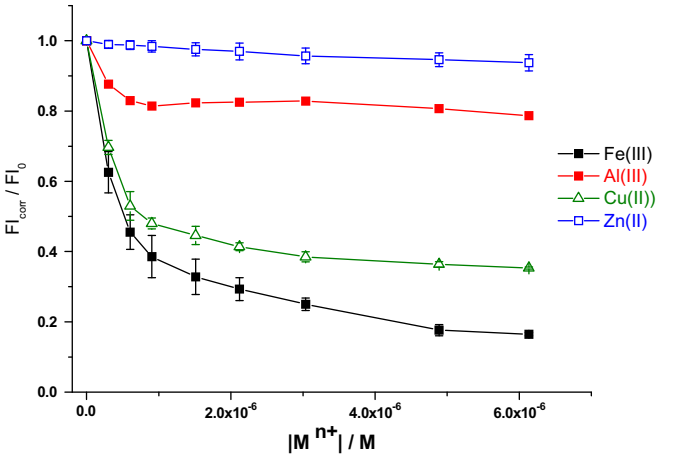

Fig. 8. Emission fluorescence intensity quenching of 3 μM **Cat1** in MOPS (10 mM, pH 7.4, 25 °C), with increasing concentrations of Fe^{3+}, Al^{3+}, Cu^{2+} and Zn^{2+}.

a different behaviour of the paramagnetic metal ions Fe^{3+} and Cu^{2+} and diamagnetic $Al^{3+}$and Zn^{2+}. The results presented in Fig. 8. are the mean values obtained in three independent experiments. From inspection of data in Fig. 8 it is clear that Al^{3+} and Zn^{2+} do not significantly influence the fluorescence intensity, whereas Fe^{3+} and Cu^{2+} have a considerable fluorescence quenching effect. Although emission fluorescence quenching of **Cat1** in the presence of Cu^{2+} is appreciable, under physiological conditions the levels of low molecular weight complexes of Cu^{2+} ($\approx 10^{-15}$ M) [35] are much lower than the ones observed for Fe^{3+} ($\approx 10^{-6}$ M) [36]. Moreover, taking these results together with the reported complex stability constants of Fe(III) and Cu(II) with catechols, 13.02 [15] and 11.5 [37], respectively, it can be expected that, in physiological conditions, the interaction between Fe(III) and **Cat1** should be more relevant when compared with Cu(II). Therefore if an emission fluorescence quenching effect of **Cat1** is observed, in living cells, this is most likely to be associated with the presence of chelatable iron and not with a Cu(II) presence.

4. Conclusions

A novel fluorescein-based dye containing a catechol chelating unit – **Cat1** – was synthesised and its photophysical properties were determined. The reported data in this work points out for a potential application of this new **Cat1** as an ion sensor in biological media, particularly for iron(III), and analytical applications of this compound are in course.

Acknowledgments

This work has been supported by Fundação para a Ciência e aTecnologia (FCT) through grant no. PEst-C/EQB/LA0006/2011. C. Queirós thanks FCT a grant through project PTDC/QUI/67915/2006. We also thank Dr. Andrea Carneiro from CENTI, V.N. Famalicão, for making available to us a CEM Discover microwave reactor. The Bruker Avance II 400 spectrometer is part of the National NMR network and was purchased under the framework of the National Programme for Scientific Re-equipment, contracREDE/1517/RMN/2005, with funds from POCI 2010 (FEDER) and (FCT). S. Lopes thanks FCT for an SFRH/BPD/34262/2006 fellowship.

Appendix. Supporting information

Supplementary material associated with this article can be found, in the online version, at doi:10.1016/j.dyepig.2011.10.010.

References

[1] Domaille DW, Que EL, Chang CJ. Synthetic fluorescent sensors for studying the cell biology of metals. Nature Chemical Biology 2008;4:168–75.
[2] Lodeiro C, Capelo JL, Mejuto JC, Oliveira E, Santos HM, Pedras B, et al. Light and colour as analytical detection tools: a journey into the periodic table using polyamines to bio-inspired systems as chemosensors. Chemical Society Reviews 2010;39:2948–76.
[3] Kim HN, Lee MH, Kim HJ, Kim JS, Yoon J. A new trend in rhodamine-based chemosensors: application of spirolactam ring-opening to sensing ions. Chemical Society Reviews 2008;37:1465–72.
[4] Fan LJ, Zhang Y, Murphy CB, Angell SE, Parker MFL, Flynn BR, et al. Fluorescent conjugated polymer molecular wire chemosensors for transition metal ion recognition and signaling. Coordination Chemistry Reviews 2009;253:410–22.
[5] Czarnik A. Chemical communication in water using fluorescent chemosensors. Accounts on Chemical Research 1994;27:302–8.
[6] Móczár I, Huszthy P, Mezei A, Kádár M, Nyitrai J, Tóth K. Synthesis and optical characterization of novel azacrown ethers containing an acridinone or an *N*-methylacridinone unit as potential fluorescent chemosensors. Tetrahedron 2010;66:350–8.
[7] Basabe-Desmonts L, Reinhoudt DN, Crego-Calama M. Design of fluorescent materials for chemical sensing. Chemical Society Reviews 2007;36:993–1017.
[8] Frade VHJ, Coutinho PJG, Moura JCVP, Gonçalves MST. Functionalised benzo[a]phenoxazine dyes as long-wavelength fluorescent probes for amino acids. Tetrahedron 2007;63:1654–63.
[9] Petrat F, De Groot H, Rauen U. Determination of the chelatable iron pool of single intact cells by laser scanning microscopy. Archives of Biochemistry and Biophysics 2000;376:74–81.
[10] Bazzicalupi C, Bencini A, Biagini S, Faggi E, Farruggia G, Andreani G, et al. A highly pH-sensitive Zn(II) chemosensor. Dalton Transactions 2010;39:7080–90.
[11] Li T, Yang Z, Li Y, Liu Z, Qi G, Wang B. A novel fluorescein derivative as a colorimetric chemosensor for detecting copper(II) ion. Dyes and Pigments 2011;88:103–8.
[12] Gonçalves MST. Fluorescent Labeling of Biomolecules with Organic probes. Chemical Reviews 2009;109:190–212.
[13] Callan JF, Silva P, Ferguson J, Huxley AJM, O'Brien AM. Fluorescent photoionic devices with two receptor and two switching mechanisms: applications to pH sensors and implications for metal ion detection. Tetrahedron 2004;60:11125–31.
[14] Motekaitis RJ, Martell AE. Complexes of aluminum(III) with hydroxy carboxylic acids. Inorganic Chemistry 1984;23:18–23.
[15] Avdeef A, Sofen SR, Bregante TL, Raymond KN. Coordination chemistry of microbial iron transport compounds. 9. Stability constants for catechol models of enterobactin. Journal of the American Chemical Society; 1978:5362–70.
[16] Nutt JG. Catechol-O-methyltransferase inhibitors for treatment of Parkinson's disease. The Lancet 1998;351:1221–2.
[17] Jobe SO, Ramadoss J, Koch JM, Jiang Y, Zheng J, Magness RR. Estradiol-17β and its cytochrome P450- and catechol-O-methyltransferase-derived metabolites stimulate proliferation in uterine artery endothelial cells. Hypertension 2010;55:1005–11.
[18] Villegas AM, Catalán LE, Venegas IM, García JV, Altamirano HC. New catechol derivatives of safrole and their antiproliferative activity towards breast cancer cells. Molecules 2011;16:4632–41.
[19] Kaim W, Schwederski B. Bioinorganic chemistry. 2 ed. Stuttgart, B.G.: Teubner; 1995.
[20] Gaboriau F, Chantrel-Groussard C, Rakba N, Loyer P, Pasdeloup N, Hider RC, et al. Iron mobilization, cytoprotection, and inhibition of cell proliferation in normal and transformed rat hepatocyte cultures by the hydroxypyridinone CP411, compared to CP20: a biological and physicochemical study. Biochemical Pharmacology 2004;67:1479–87.
[21] Fakih S, Podinovskaia M, Kong X, Schaible UE, Collins HL, Hider RC. Monitoring intracellular labile iron pools: a novel fluorescent iron(III) sensor as a potential non-invasive diagnosis tool. Journal of Pharmaceutical Sciences 2009;98:2212–26.
[22] Ma Y, De Groot H, Liu Z, Hider RC, Petrat F. Chelation and determination of labile iron in primary hepatocytes by pyridinone fluorescent probes. Biochemistry Journal 2006;395:49–55.
[23] Fakih S, Podinovskaia M, Kong X, Collins HL, Schaible UE, Hider RC. Targeting the lysosome: fluorescent iron(III) chelators to selectivity monitor endosomal/lysosomal labile iron pools. Journal of Medicinal Chemistry 2008;51:4539–52.
[24] Gans P, Sabatini A, Vacca A. Investigation of equilibria in solution. Determination of equilibrium constants with the HYPERQUAD suite of programs. Talanta 1996;43:1739–53.
[25] Albert A, Sergeant EP. The determination of ionization constants. 2 ed. London: Chapman & Hall; 1971.

[26] Alderighi L, Gans P, Ienco A, Peters D, Sabatini A, Vacca A. Hyperquad simulation and speciation (HySS): a utility program for the investigation of equilibria involving soluble and partially soluble species. Coordination Chemistry Reviews 1999;184:311–8.
[27] Williams ATR, Winfield SA, Miller JN. Relative fluorescence quantum yields using a computer-controlled luminescence spectrometer. Analyst 1983;108: 1067–71.
[28] Fery-Forgues S, Lavabre D. Are fluorescence quantum yields so tricky to measure? A demonstration using familiar stationery products. Journal of Chemical Education 1999;76:1260–4.
[29] Baoyan W, Xiaoling G, Yulin H, Zhixing S. Synthesis and photophysical behavior of a water-soluble fluorescein-bearing polymer for Fe^{3+} ion sensing. Journal of Polymer Research 2008;15:427–33.
[30] Lakowicz JR. Principles of fluorescence spectroscopy. 3 ed. Berlin, Heidelberg: Springer; 2006.
[31] Dubé D, Scholte AA. Reductive N-alkylation of amides, carbamates and ureas. Tetrahedron Letters 1999;40:2295–8.
[32] Leite A, Silva AMG, Nunes A, Andrade M, Sousa C, Cunha-Silva L, et al. Novel tetradentate chelators derived from 3-hydroxy-4-pyridinone units: synthesis, characteization and aqueous solution properties. Tetrahedron 2011;67: 4009–16.
[33] McKinney RM, Churchill II FC. Reaction paths to pure 5- and 6-aminofluorescein. Pitfalls encountered in conventional synthesis procedures. Journal of the Chemical Society C: Organic 1970;5:654–6.
[34] Sjöback R, Nygren J, Kubista M. Absorption and fluorescence properties of fluorescein. Spectrochimica Acta Part A: Molecular and Biomolecular Spectroscopy 1995;51:L7–21.
[35] Rae TD, Schmidt PJ, Pufahl RA, Cullota VC, O'Halloran TV. Undetectable intracellular free copper: the requirement of a copper chaperone for superoxide dismutase. Science 1999;284:805–8.
[36] Glickstein H, El RB, Shvartsman M, Cabantchik ZI. Intracellular labile iron pools as direct targets of iron chelators: a fluorescence study of chelator action in living cells. Blood 2005;106:3242–50.
[37] Balla J, Kiss T, Jameson RF. Copper(II)-catalyzed oxidation of catechol by molecular oxygen in aqueous solution. Inorganic Chemistry 1992;31:58–62.